Continuum Opacity, Partial Frequency Redistribution, and Molecular Line Contamination

Han Uitenbroek
National Solar Observatory/Sacramento Peak
Sunspot, USA

Hale COLLAGE, Boulder, Feb 25, 2016

Continuum processes

Outside spectral lines the solar plasma has significant opacity in so called continuum processes. They are called this way because their opacity varies very slowly with wavelength. Major examples are:

- Atomic Bound–free and free–free transitions.
- H^- bound–free and free-free.
- Thomson scattering off free electrons.
- Rayleigh scattering off atoms (mainly hydrogen and helium)

Bound–Free Cross Sections of Hydrogen

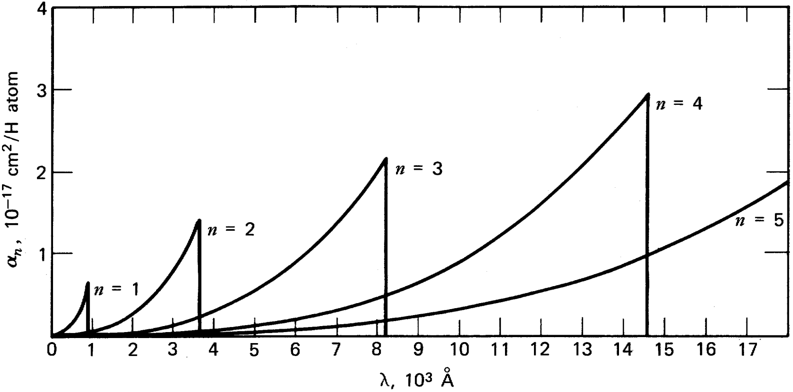

H^- Opacity

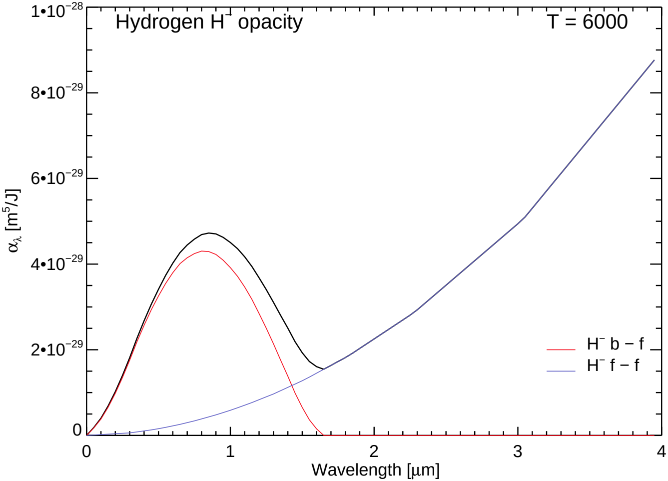

$$\Delta E^{\mathrm{bf}} = 0.754 \text{ eV}$$

Temperature Sensitivity of H^- Opacity

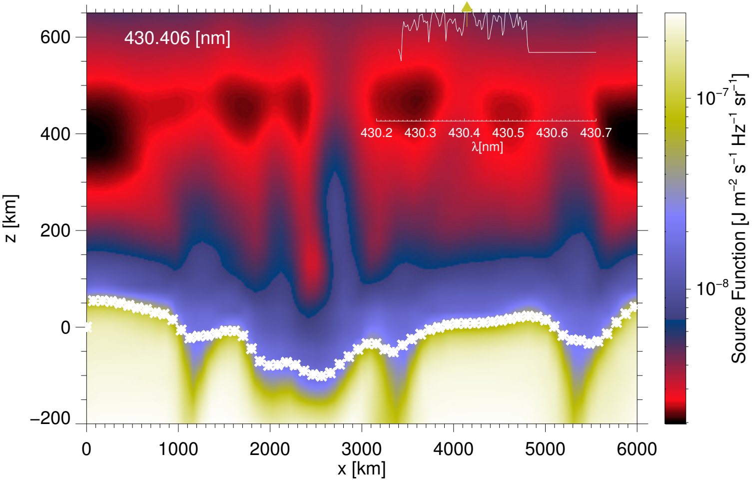

Background Scattering Processes

Thomson scattering (non-relativistic):

$$\alpha_e^T = N_e \sigma_e = N_e \frac{8\pi}{3 m_e^4 c^2} \frac{q_e^4}{(4\pi\epsilon_0)^2}$$

Rayleigh scattering:

$$\alpha^R(\omega) = \sigma_e f_{ij} \omega^4 / (\omega_{ij}^2 - \omega^2)^2$$

Linear Polarization towards the Limb:

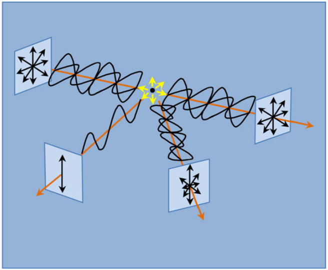

Linear Sacttering Polarization at 400 nm

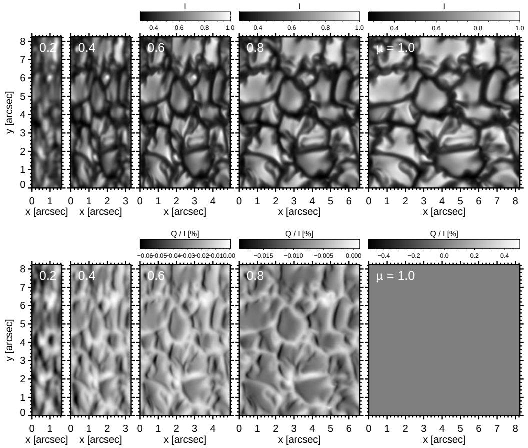

Relative Contributions to the Background at 400 nm

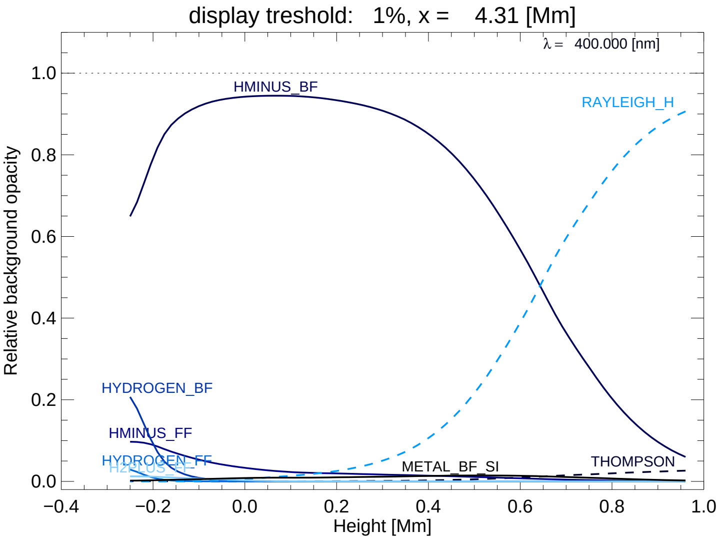

Frequency Redistribution

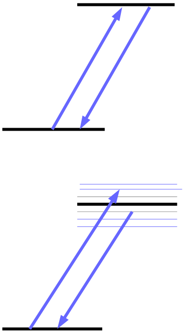

Ca II H and K lines

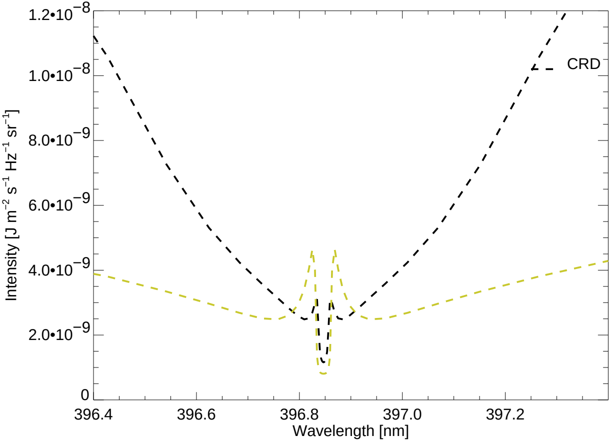

Ca II H and K lines

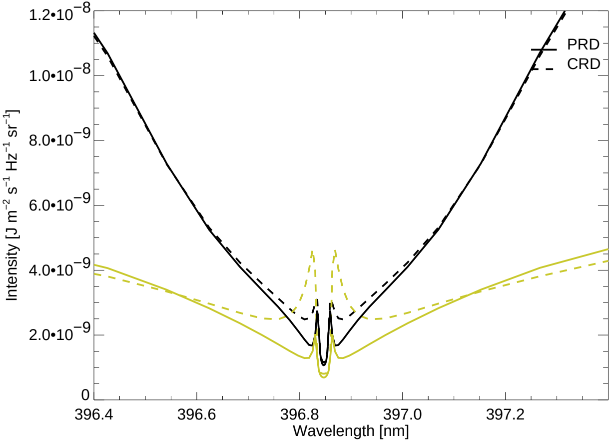

Ca II H and K lines

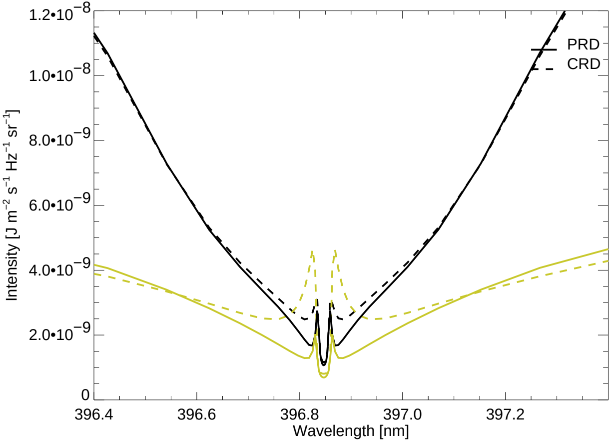

Mg II h and k lines

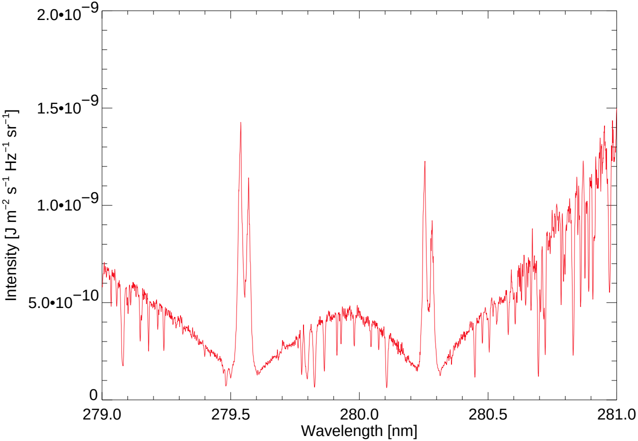

Mg II h and k lines

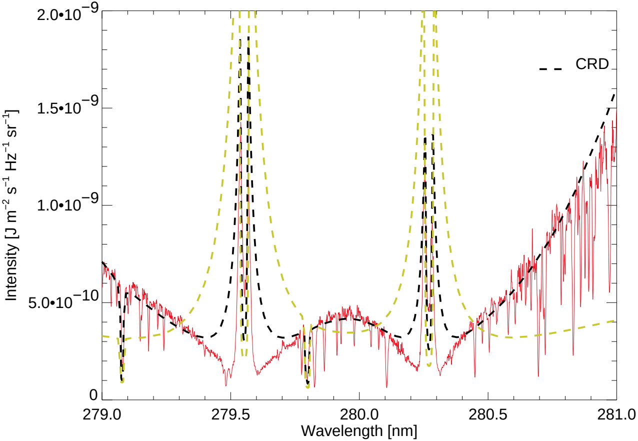

Mg II h and k lines

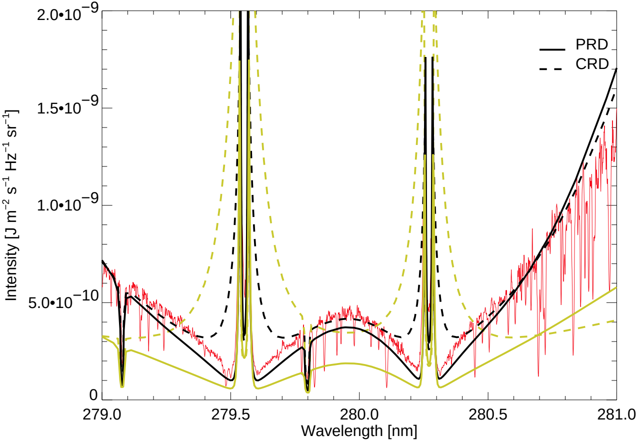

Mg II h and k lines

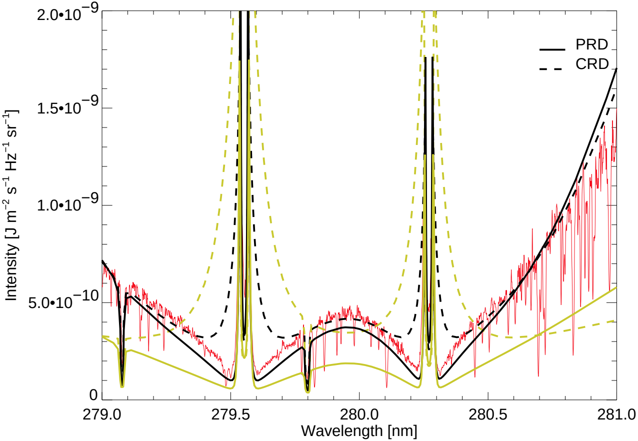

Hydrogen Lyman–α profiles

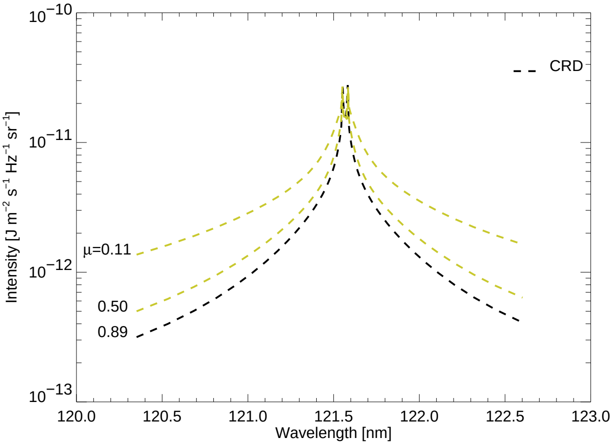

Hydrogen Lyman–α profiles

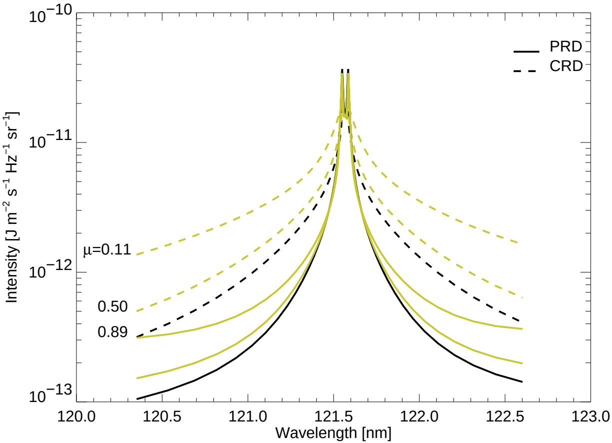

Hydrogen Lyman–α profiles

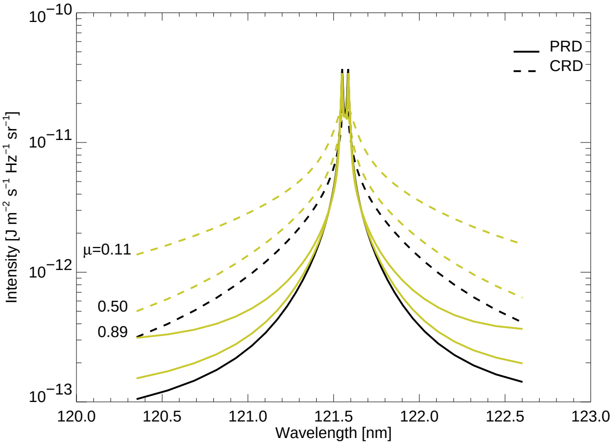

The Redistribution Function R_{ij}

References: Hummer (1962), Heinzel & Hubeny (1982)

The laboratory frame redistribution function:

$$R_{ij}(\nu, \mathbf{n}; \nu', \mathbf{n}') d\nu d\nu' \frac{d\Omega}{4\pi} \frac{d\Omega'}{4\pi}$$

Describes the conditional probablility that, when a photon in line (i, j) and solid angle $d\Omega'$ around direction $\mathbf{n}'$ and frequency range $(\nu', \nu' + d\nu')$ is scattered by that line, it will be emitted into angle $d\Omega$ around direction $\mathbf{n}$ and frequency range $(\nu, \nu + d\nu)$.

Complete frequency in the laboratory frame:

$$R_{ij}^{\mathrm{incoh}}(\nu, \mathbf{n}; \nu', \mathbf{n}') = \phi_{ij}(\nu, \mathbf{n}) \phi_{ij}(\nu', \mathbf{n}')$$

The Redistribution Function R_{ij} (2)

Normalization:

$$\oint\oint \frac{d\Omega}{4\pi}\frac{d\Omega'}{4\pi}\int\int d\nu' d\nu \; R_{ij}(\nu, \mathbf{n}; \nu', \mathbf{n}') \equiv 1$$

$$\oint \frac{d\Omega'}{4\pi}\int d\nu' \; R_{ij}(\nu, \mathbf{n}; \nu', \mathbf{n}') \equiv \phi_{ij}(\nu, \mathbf{n})$$

Coherency fraction:

$$R_{ij} = \gamma R_{ij}^{\mathrm{coh}} + (1-\gamma) R_{ij}^{\mathrm{incoh}}$$

$$\gamma = P_j / (P_j + Q_{\mathrm{E}})$$

Partial Frequency Redistribution in the emission profile

$$\psi_{ij}^{\mathrm{PRD}}(\nu) = \phi_{ij}(\nu) \left\{ 1 + \gamma \frac{n_i B_{ij}}{n_j P_j} \int \left[\frac{R_{iji}^{I}(\nu, \nu')}{\phi_{ij}(\nu)} - \phi_{ij}(\nu') \right] J(\nu') d\nu' \right\}$$

O I resonance triplet

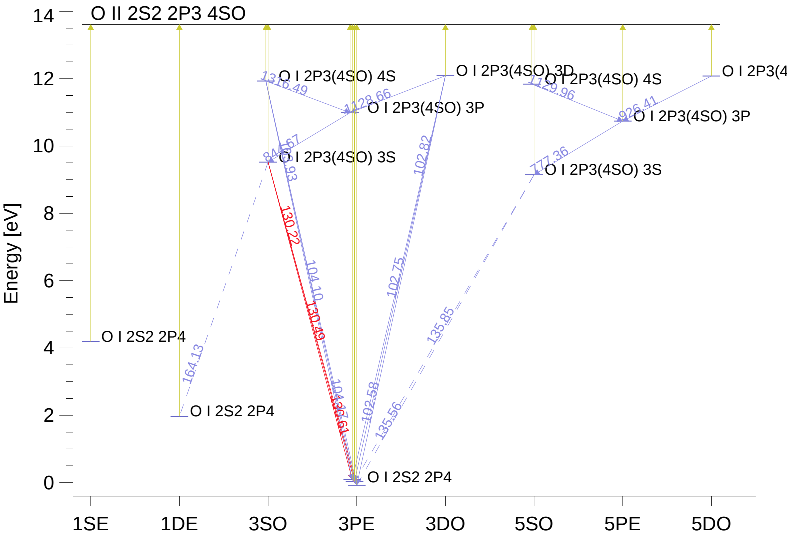

O I triplet: CRD and PRD compared to HRTS

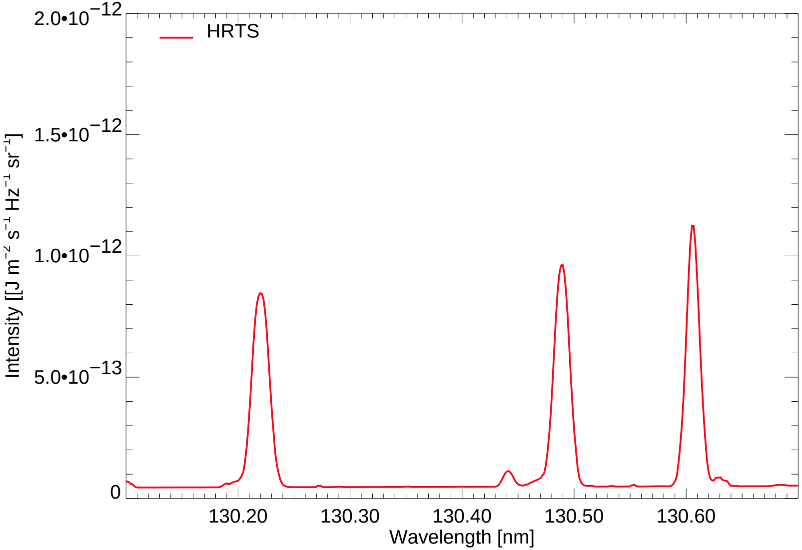

O I triplet: CRD and PRD compared to HRTS

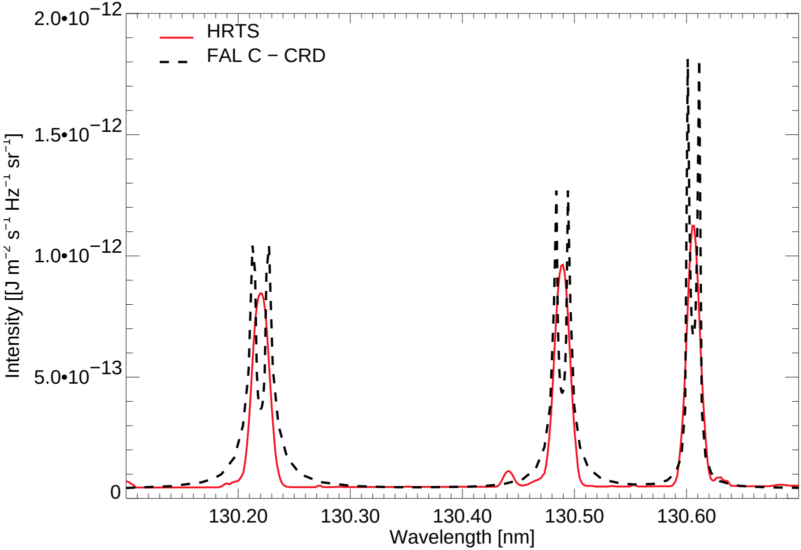

O I triplet: CRD and PRD compared to HRTS

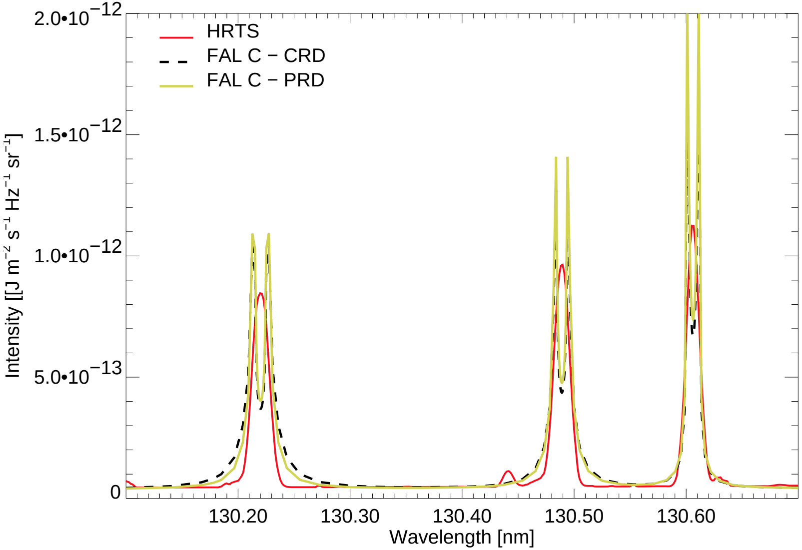

O I triplet: CRD and PRD compared to HRTS

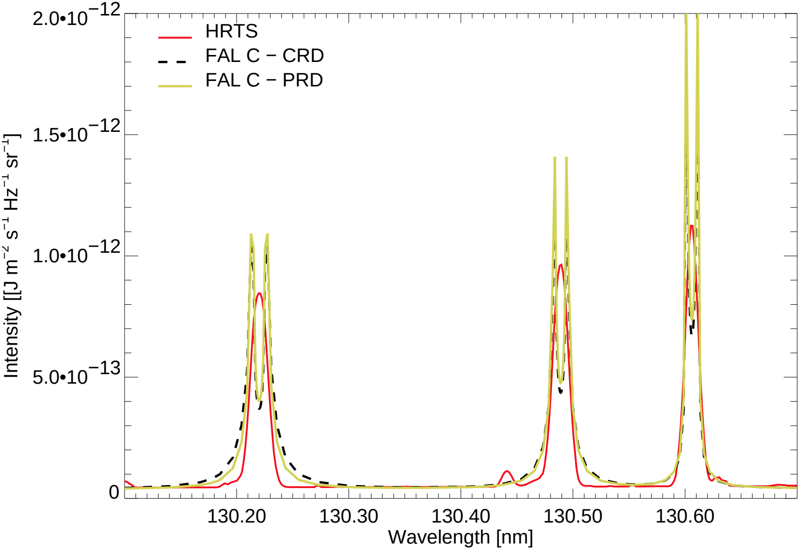

Cross-redistribution XRD

$$\frac{\psi_{ij}^{\mathrm{PRD}}(\nu)}{\phi_{ij}(\nu)} = 1 + \gamma \sum_{k<j} \frac{n_k B_{kj}}{n_j P_j} \int \left[\frac{R_{kji}^{I}(\nu, \nu')}{\phi_{ij}(\nu)} - \phi_{kj}(\nu') \right] J(\nu') d\nu'$$

Cross-redistribution XRD

$$\frac{\psi_{ij}^{\mathrm{PRD}}(\nu)}{\phi_{ij}(\nu)} = 1 + \gamma \sum_{k<j} \frac{n_k B_{kj}}{n_j P_j} \int \left[\frac{R^{I}_{kji}(\nu, \nu')}{\phi_{ij}(\nu)} - \phi_{kj}(\nu') \right] J(\nu') d\nu'$$

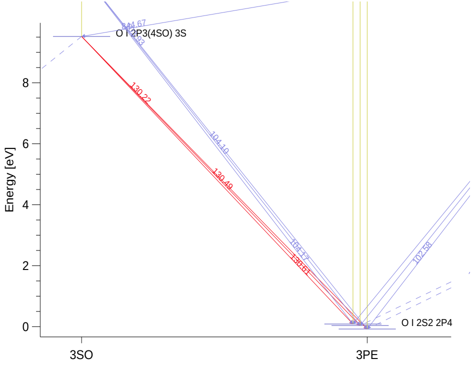

O I triplet: PRD in one line

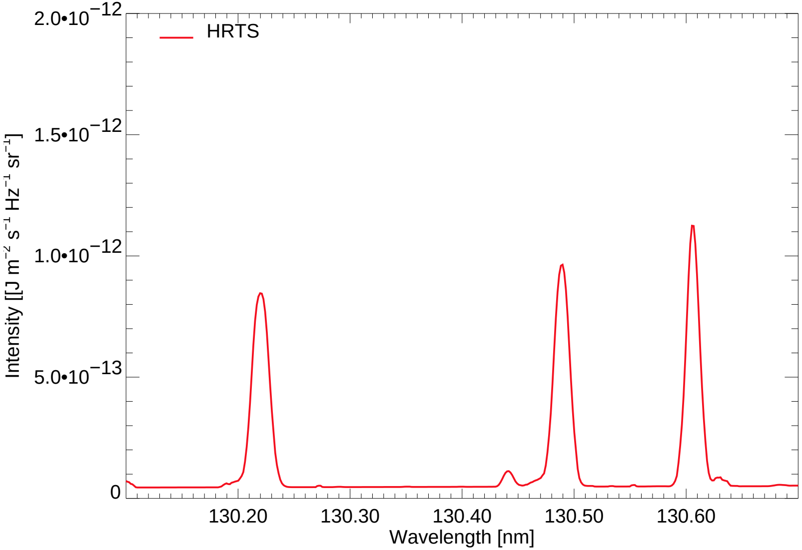

O I triplet: PRD in one line

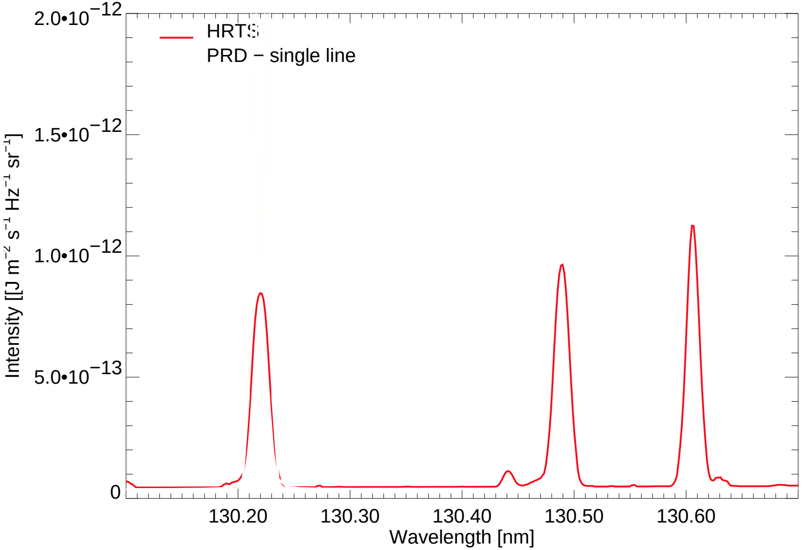

O I triplet: PRD in one line

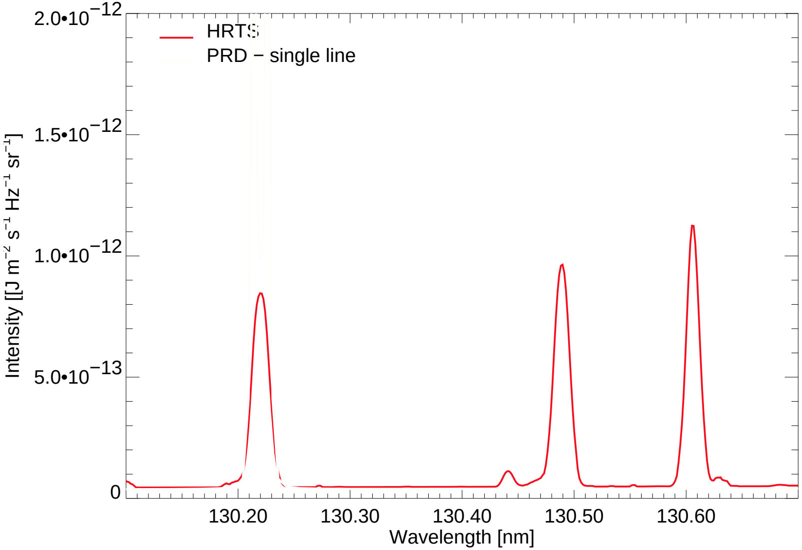

O I resonance triplet: XRD

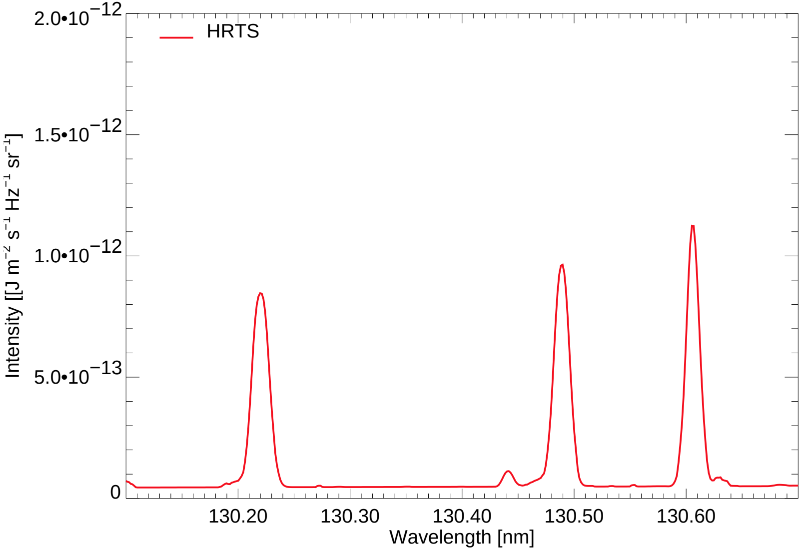

O I resonance triplet: XRD

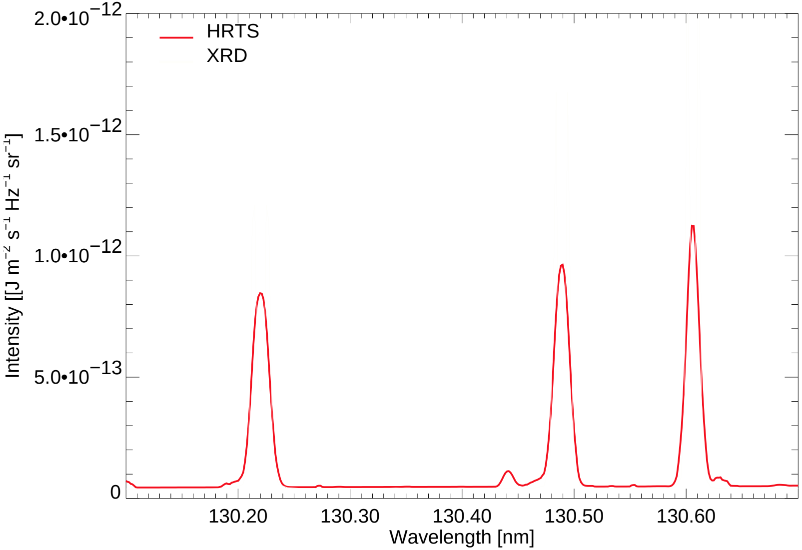

O I resonance triplet: XRD

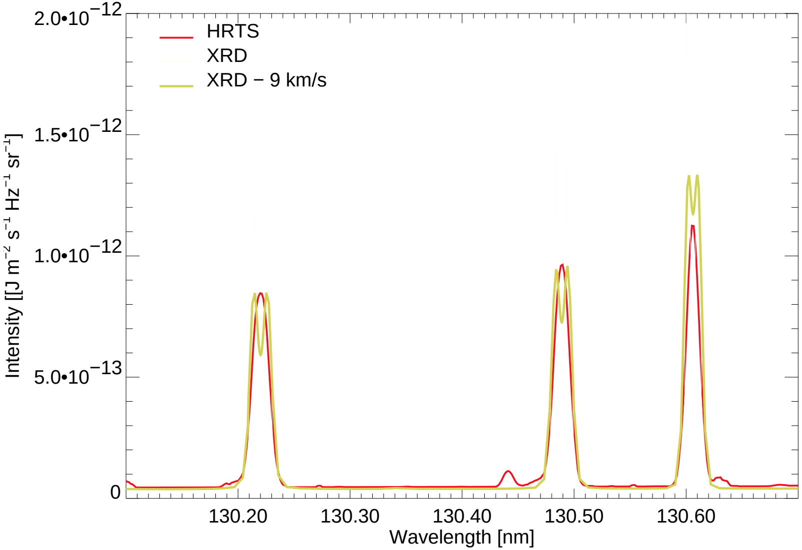

O I resonance triplet: XRD

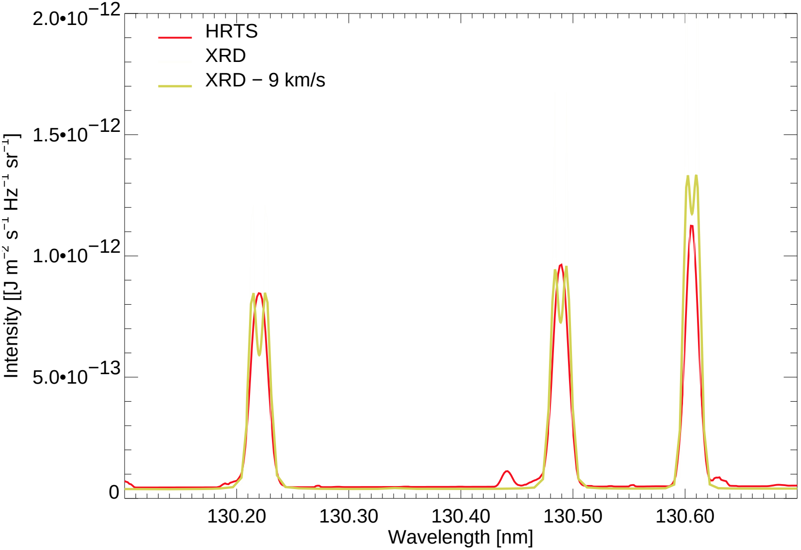

Using Doppler shift to measure photospheric velicities

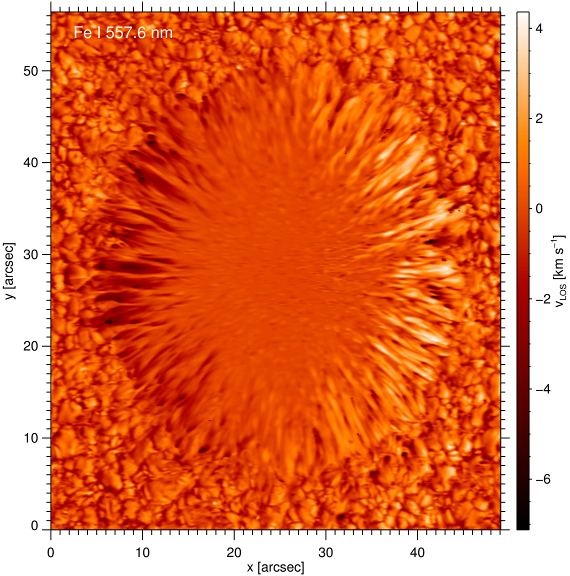

Spectrum around Fe I 557.6 nm

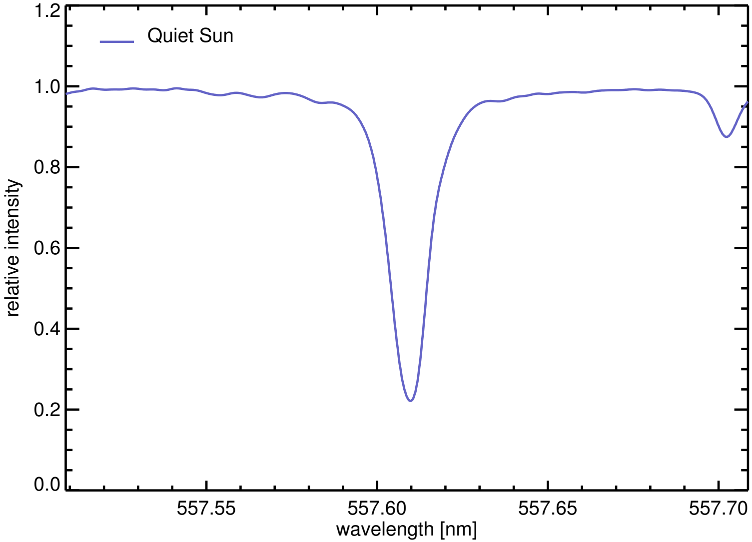

Spectrum around Fe I 557.6 nm

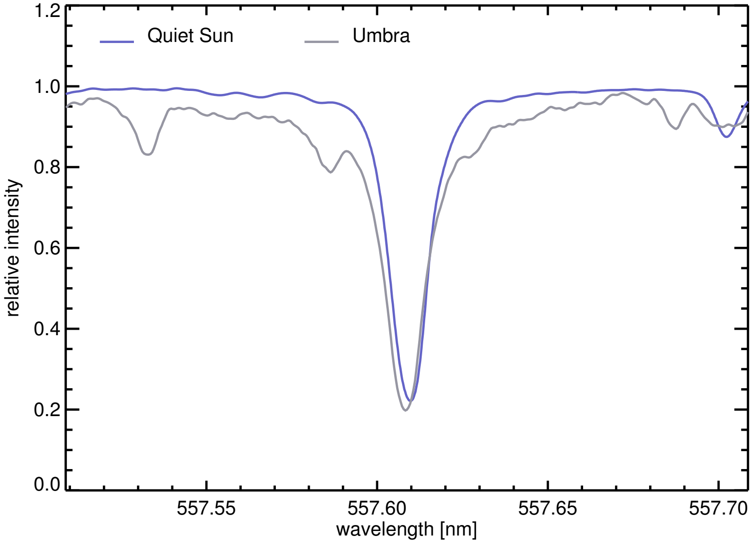

Spectrum around Fe I 557.6 nm

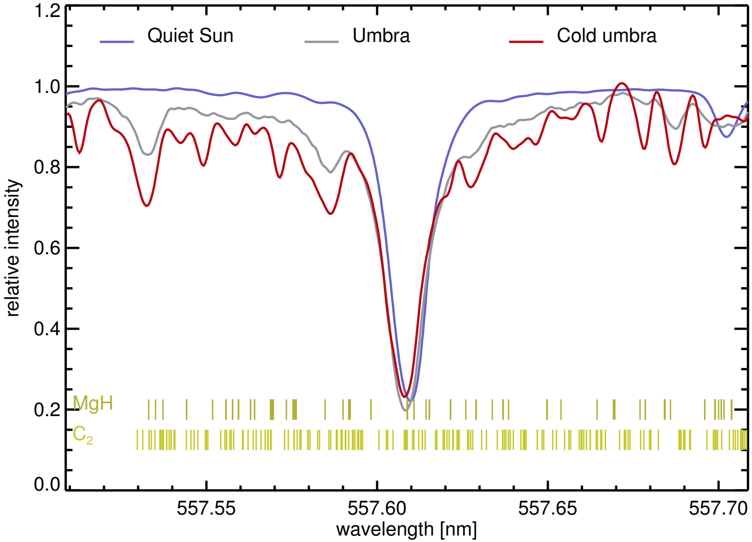

Spectrum around Fe I 557.6 nm

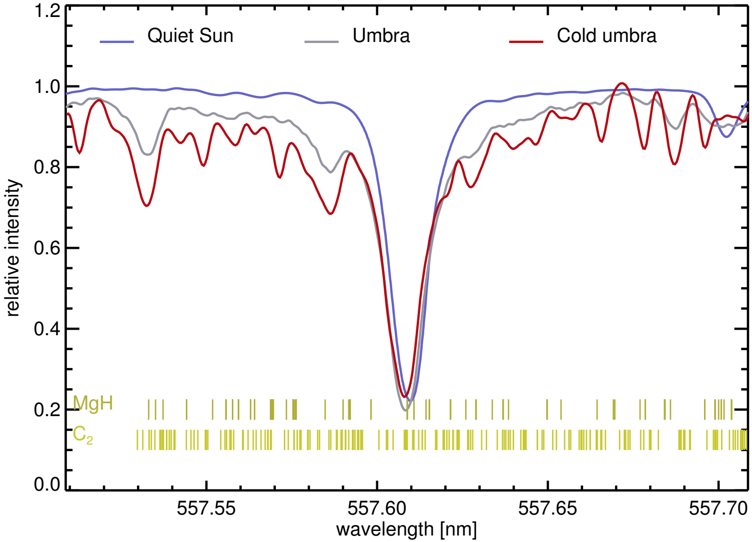

Spectrum around C I 538.0 nm

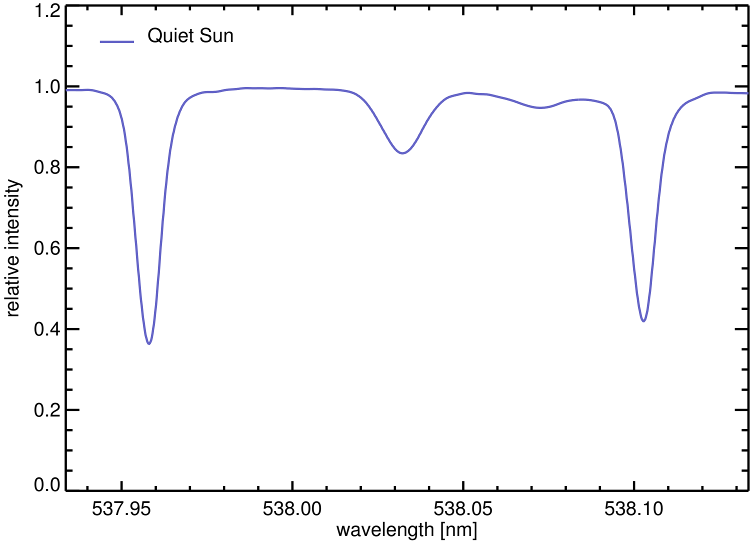

Spectrum around C I 538.0 nm

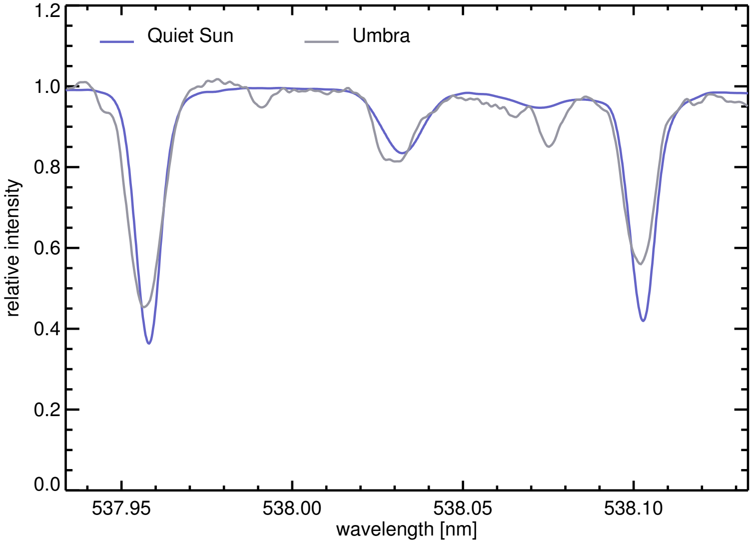

Spectrum around C I 538.0 nm

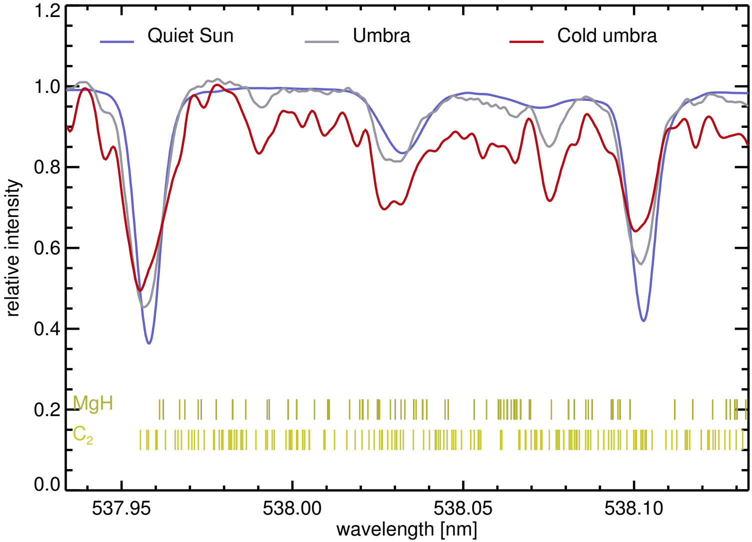

Spectrum around C I 538.0 nm

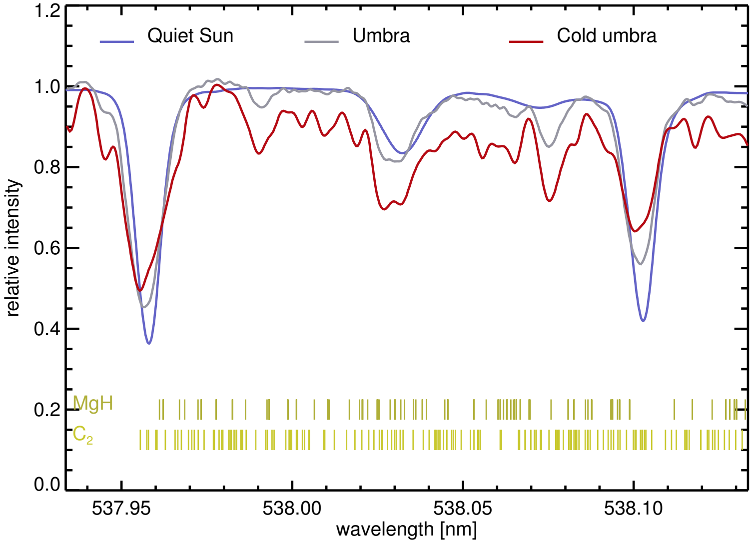

Stokes spectrum C I 538.0 nm

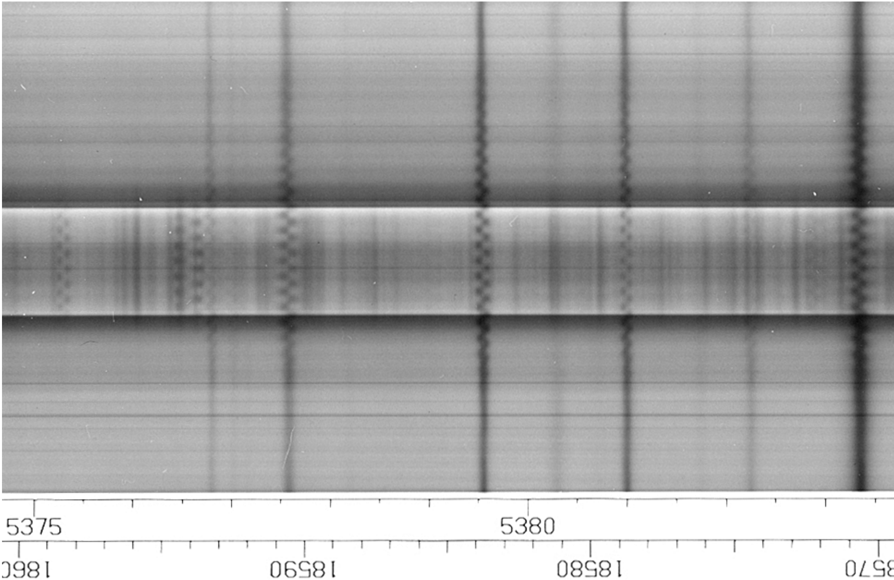

Spectrum around Fe I 709.0 nm

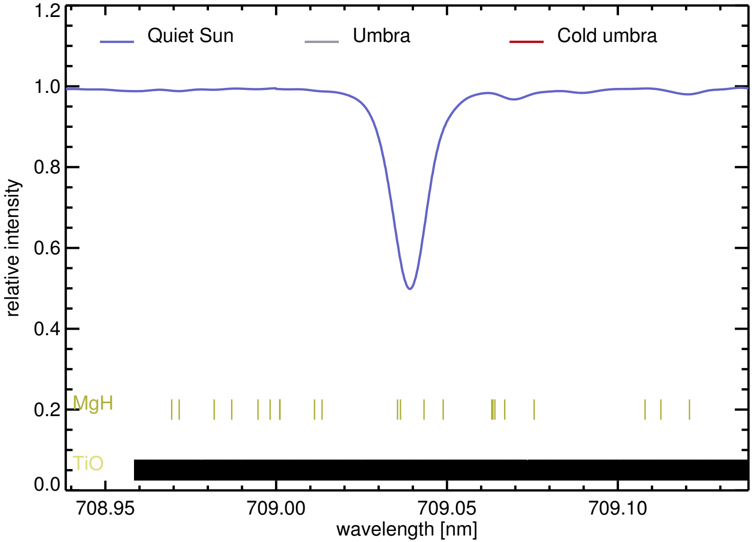

TiO lines around Fe I 617.3 nm

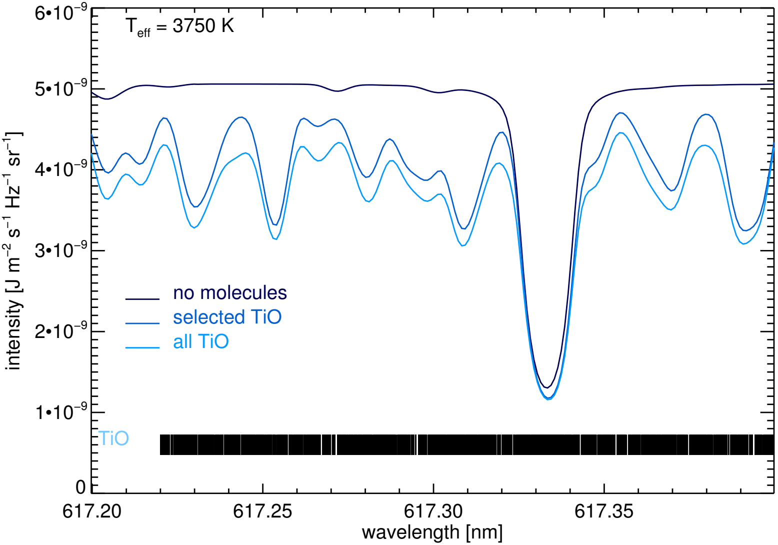

One-dimensional models

- Radiative equilibrium models (Kurucz) with different effective temperatures: 3750 – 6250 K.

One-dimensional models

- Radiative equilibrium models (Kurucz) with different effective temperatures: 3750 – 6250 K.
- LTE source functions and opacities.

One-dimensional models

- Radiative equilibrium models (Kurucz) with different effective temperatures: 3750 – 6250 K.
- LTE source functions and opacities.
- Chemical equilibrium (Saha–Boltzmann).

One-dimensional models

- Radiative equilibrium models (Kurucz) with different effective temperatures: 3750 – 6250 K.
- LTE source functions and opacities.
- Chemical equilibrium (Saha–Boltzmann).

C I 538.0 nm line at different effective temperatures

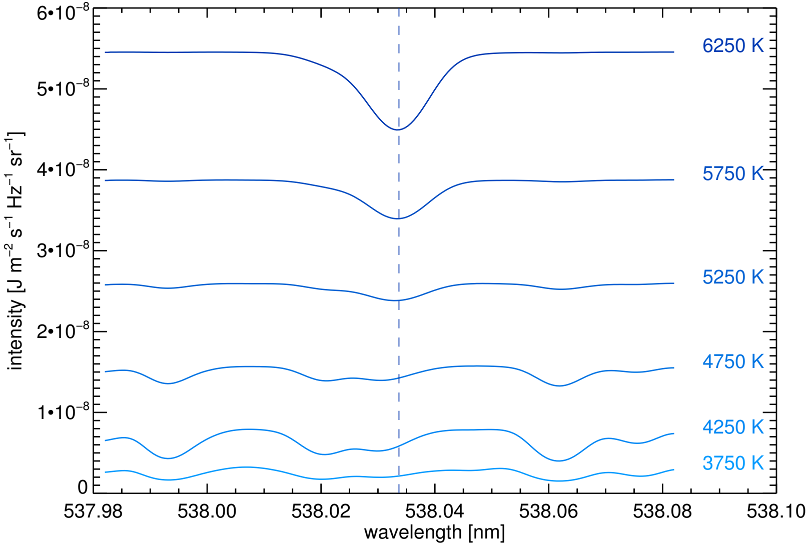

Fe I 709.0 nm line at different effective temperatures

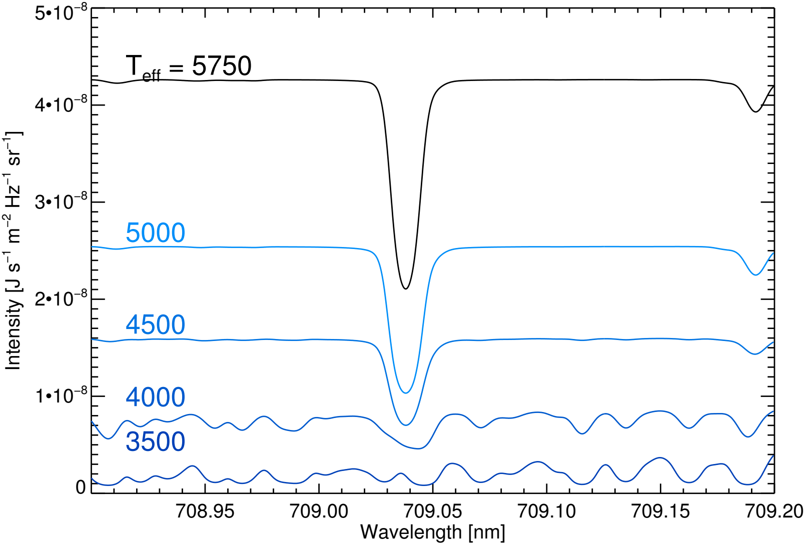

Relative concentration of MgH molecules

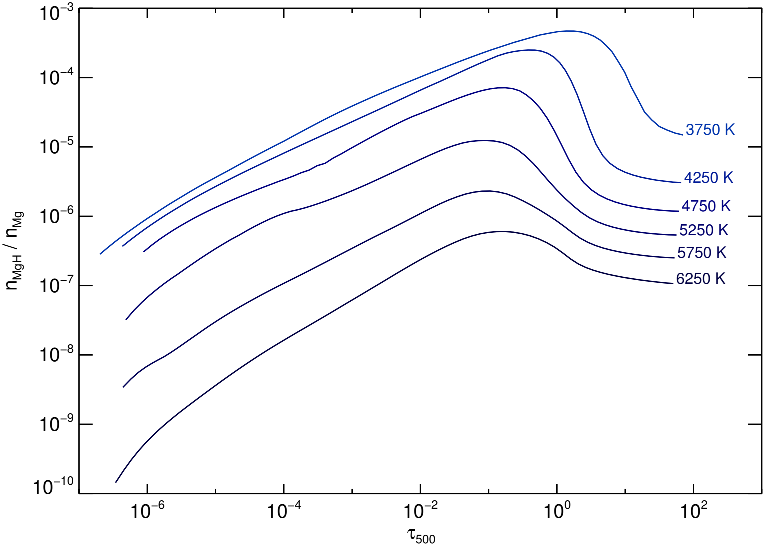

Relativ concentration of C_2 and CO molecules

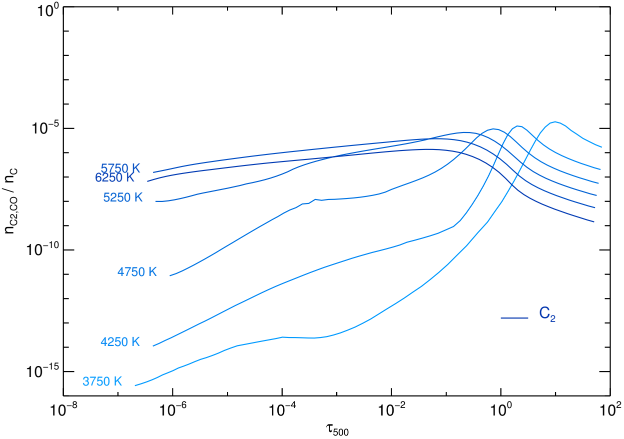

Relativ concentration of C_2 and CO molecules

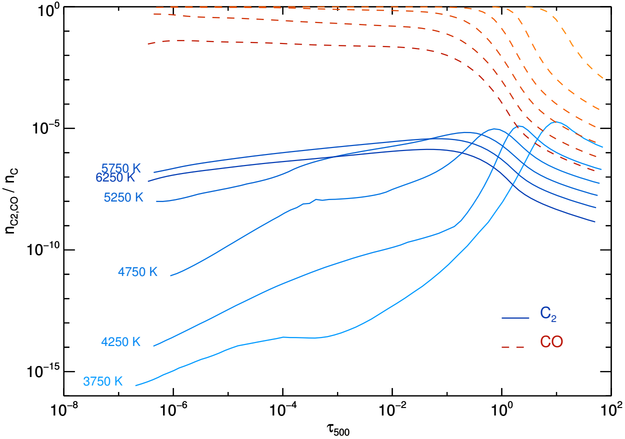

Relativ concentration of C_2 and CO molecules

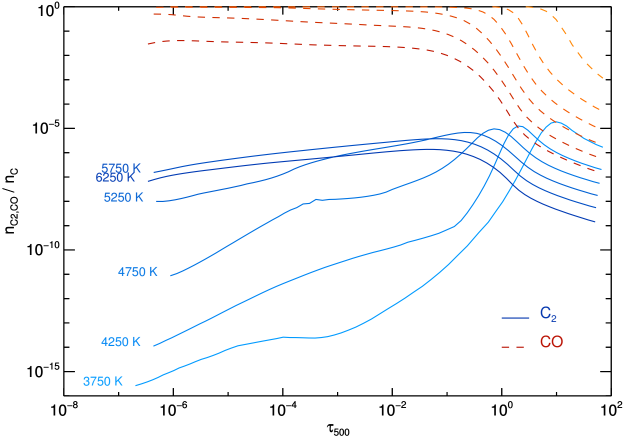

Measuring velocities from bisectors

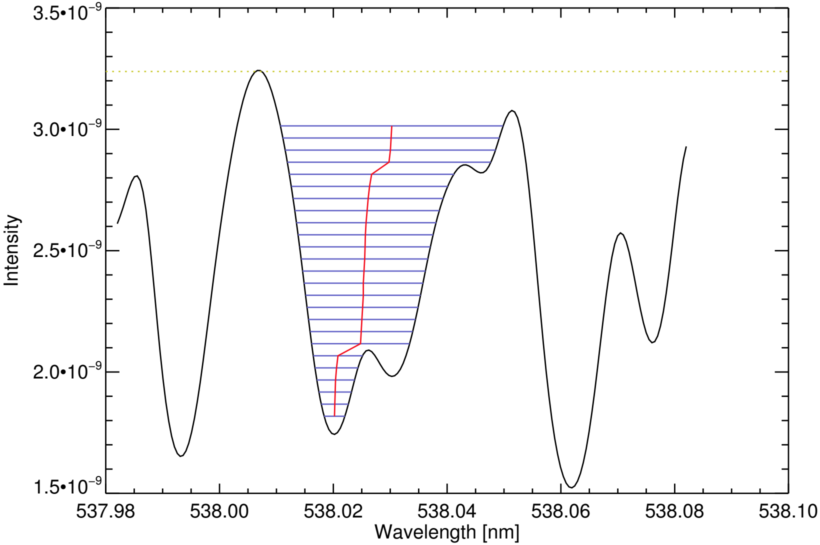

Bisectors of C I 538.0 nm at different T_{eff}

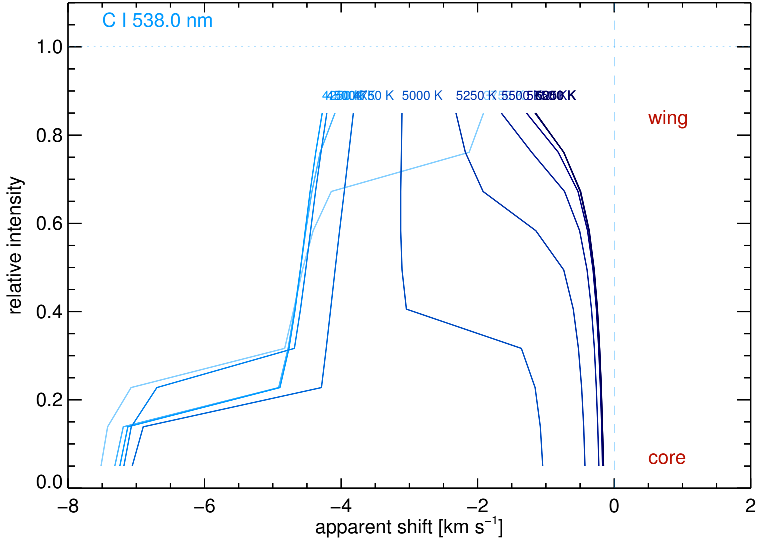

Apparent shift of Fe I 557.6 nm in Sunspot: core

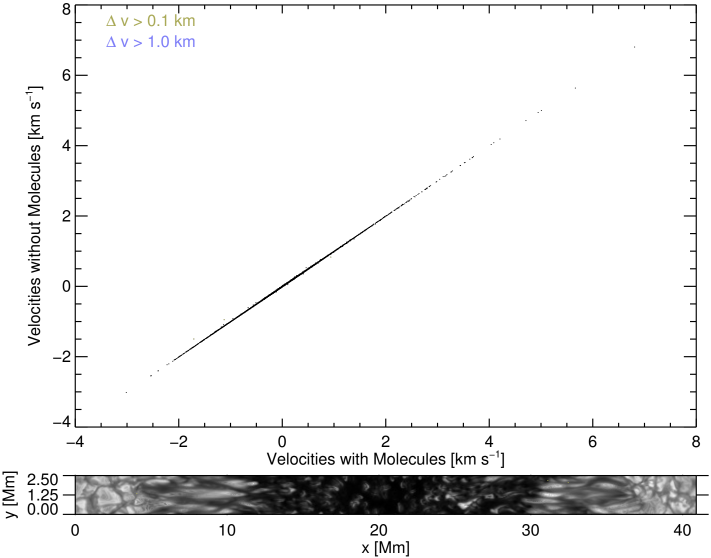

Apparent shift of Fe I 557.6 nm in Sunspot: half-max

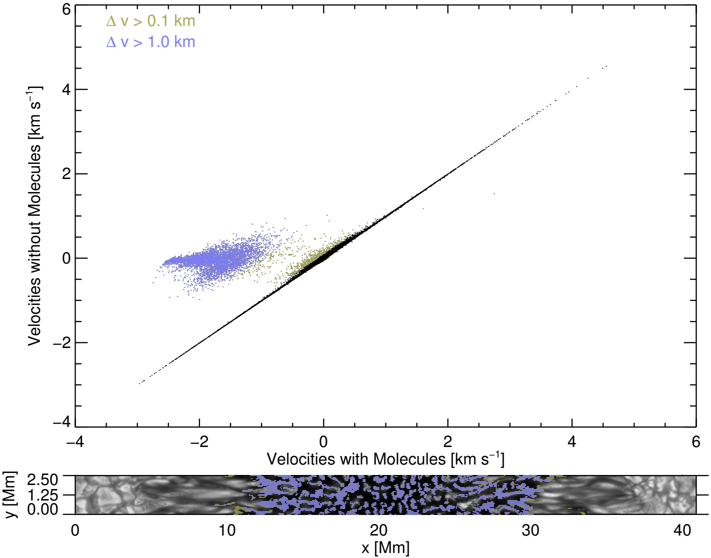

Apparent shift of Fe I 557.6 nm in Sunspot: wing

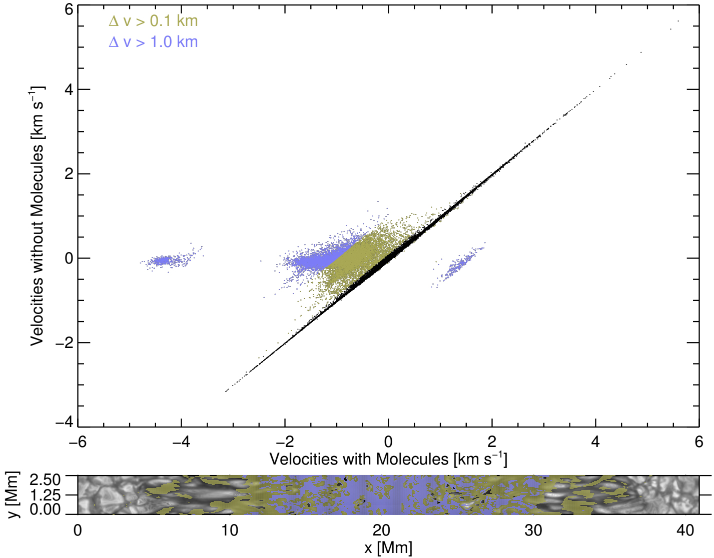

Apparent shift of C I 538.0 nm in Sunspot: core

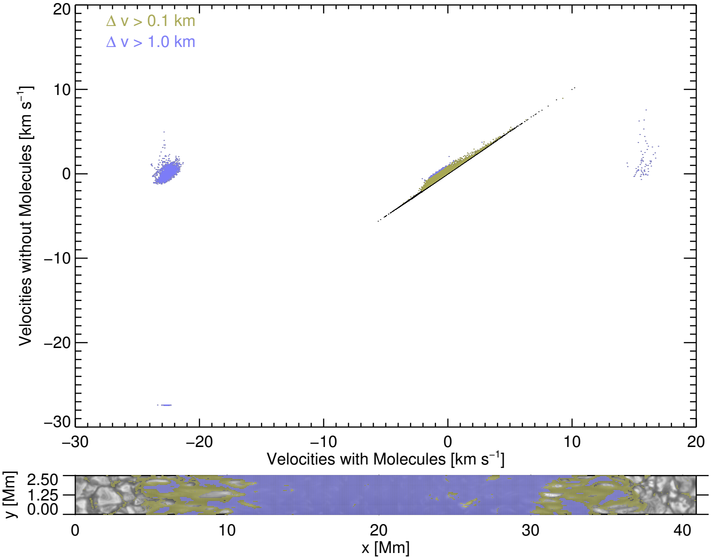

Apparent shift of C I 538.0 nm in Sunspot: wing